

Long non-coding RNA TUG1 regulates the progression and metastasis of osteosarcoma cells *via* miR-140-5p/PFN2 axis

Z.-Y. ZHAO¹, Y.-C. ZHAO¹, W. LIU²

¹Department of Osteoarthropathy, Yantai Hospital, Zhifu, Yantai, Shandong, China

²Department of Pathophysiology, Binzhou Medical University, Yantai, Shandong, China

Abstract. – OBJECTIVE: Osteosarcoma (OS) is a frequently occurred tumor. Recently, increasing reports disclosed that long non-coding RNA taurine upregulated gene 1 (TUG1) was associated with OS development. Nevertheless, the precise regulatory pattern was not completely understood. Hence, we aimed to investigate the biological role of TUG1 in OS tumorigenesis.

PATIENTS AND METHODS: The levels of TUG1, microRNA-140-5p (miR-140-5p), and Profilin 2 (PFN2) were measured via quantitative Real Time-Polymerase Chain Reaction (qRT-PCR), and the protein level of PFN2 was assessed using Western blot. In addition, MTT assay was employed to detect the ability of cell proliferation in MG63 and U2OS cells. Cell migration and invasion were estimated adopting transwell assay. Moreover, the Dual-Luciferase reporter assay was performed to verify the interrelation between miR-140-5p and TUG1 or PFN2.

RESULTS: TUG1 and PFN2 levels were evidently upregulated in OS tissues and cell lines. The knockdown of either TUG1 or PFN2 could restrain cell proliferation, migration, and invasion in OS cells. In addition, miR-140-5p was a target of TUG1 to regulate PFN2. The functions of PFN2 knockdown in cell behaviors were rescued after co-transfection with either miR-140-5p inhibitor or overexpression vector of TUG1. Importantly, TUG1 silencing could impede tumor progression *in vivo*.

CONCLUSIONS: TUG1 modulated cell proliferation, migration, and invasion via miR-140-5p/PFN2 axis in OS progression, which might trigger the development of therapeutic strategies for the treatment of OS.

Key Words:

TUG1, MiR-140-5p, PFN2, OS, Cell progression, Migration and invasion.

Introduction

Osteosarcoma (OS) is a type of solid tumor with high mortality and malignancy¹. According

to the statistics in China, around 28,000 new bone malignancy cases occurred, and about 20,700 died from bone diseases in 2015². Recently, because of the continuous development of the therapeutic strategies, the 5-year survival rate of OS patients without metastasis has significantly improved³. However, the long-term-survival of OS remains unsatisfactory^{4,5}. Thus, it is necessary to further look for novel therapeutic strategies of OS.

Long non-coding RNAs (lncRNAs), one type of the non-coding RNAs (ncRNAs), consist of more than 200 nucleotides (nts)^{6,7}. Over the past decades, lncRNAs have been disclosed to be involved in normal development and carcinogenesis^{8,9}. For example, nuclear paraspeckle assembly transcript 1 (NEAT1)¹⁰ and growth arrest-specific transcript 5 (GAS5)¹¹ have been reported to participate in the pathogenesis and tumorigenesis in OS, showing the changes of cell growth and metastasis. Young et al¹² suggests that taurine upregulated gene 1 (TUG1) is composed of 6.7-kb nts, and the imbalance of TUG1 is related to the occurrence of several cancers, such as gastric¹³, hepatocellular carcinoma¹⁴, and OS¹⁵. To be specific, the high expression of TUG1 is concerned with chemotherapy resistance in esophageal squamous cell carcinoma¹⁶. TUG1 deficiency can restrain cellular proliferation and invasion by targeting microRNA-153 in OS¹⁷. However, the biological role of TUG1 in OS tumorigenesis is still needed to be highlighted.

MicroRNAs (miRNAs) are a kind of candidate for gene therapy approaches. Their dysregulation can be regarded as the indicators of the diagnosis and prognosis in diverse cancers^{18,19}. Nevertheless, the impacts of miRNAs on OS pathogenesis and progression are different, a series of miRNAs are highly expressed, but some miRNAs, such as miR-424-5p, miR-29b, and miR-16, are evidently reduced in OS tissues. Thus, it was challenged

to identify the specific roles of miRNAs in OS²⁰. MiR-140-5p, as a member of miRNAs, has been proved to reduce the growth of ovarian cancer²¹. Besides, miR-140-5p also mediates cell proliferation and apoptosis by regulating histone deacetylase 4 (HDAC4) in OS cells. By far, whether TUG1 can modulate cell behaviors, such as proliferation and invasion *via* sponging miR-140-5p, is still ambiguous. To date, profilin 2 (PFN2) has been identified to be one of the most common profilin in mammalian cells, and it can directly interact with actin²². Based on the previous study²³, PFN2 contributes to the metastasis of colorectal cancer cells. Hence, it is necessary to understand the potential role of PFN2 in OS progression.

In this report, we aimed to research the expression patterns of TUG1, miR-140-5p, and PFN2 in OS. Also, the complex interaction between miR-140-5p and TUG1 or PFN2 was clarified. Above all, this paper expounded a novel working pathway of TUG1 in the process of OS.

Patients and Methods

Patient Tissues and Cell Culture

OS tumor tissues were obtained from 30 patients who were diagnosed with primary OS and treated at the Yantai Shan Hospital. Besides, the normal tissues (n=30) were derived from patients who have been amputated by other diseases. All the participators signed the written informed consent before this study. This research received the approval of the Ethics Committee of the Yantai Shan Hospital.

Human OS cell lines (MG63 and U2OS) and control cells (hFOB1.19) were purchased from American Type Culture Collection (ATCC; Manassas, MA, USA). Among these, MG63 cells were cultured with Eagle's Minimum Essential Medium (EMEM; ATCC, Manassas, MA, USA), U2OS cells were incubated with McCoy's 5a (Modified) Medium (Thermo Fisher Scientific, Waltham, MA, USA), and hFOB1.19 cells were grown in the mixture (1:1) of Ham's F12 Medium and Dulbecco's Modified Eagle's Medium (DMEM; Thermo Fisher Scientific, Waltham, MA, USA). It was worth noting that all the mediums needed to be added 10% fetal bovine serum (FBS; Gibco, Rockville, MD, USA) and 1'Penicillin and Streptomycin (Gibco; 100 U/mL penicillin and 100 µg/mL streptomycin). Next, the cells were cultured in a humid atmosphere with 5% CO₂ at 37°C.

Transient Transfection

All the vectors used in the study were listed: small hairpin RNA (shRNA) against TUG1 (sh-TUG1) and its negative control (sh-NC), small interfering RNA (siRNA) against TUG1 (si-TUG1) and PFN2 (si-PFN2), and their negative control (si-NC), overexpression vectors of TUG1 (pcDNA-TUG1) and PFN2 (pcDNA-PFN2), and their blank control (pcDNA-con). Besides, miR-140-5p mimic (miR-140-5p) and inhibitor (anti-miR-140-5p), as well as relative controls (miR-NC for mimic and anti-miR-NC for inhibitor), were designed in Sangon Biotechnology (Shanghai, China). The vectors and oligonucleotides were introduced into the cells by using Lipofectamine 2000 reagent (Invitrogen, Carlsbad, CA, USA) in the light of specifications.

Quantitative Real-Time Polymerase Chain Reaction (qRT-PCR) Assay

The total RNA was extracted and purified from tissues (OS and non-tumor samples) and cells (MG63, U2OS, and hFOB1.19) using TRIzol reagent (Thermo Fisher Scientific, Waltham, MA, USA). The primers of TUG1, miR-140-5p, PFN2, glyceraldehyde-3-phosphate dehydrogenase (GAPDH), and U6 were synthesized in Sangon Biotechnology (Shanghai, China). High Capacity cDNA Reverse Transcription Kit (Applied Biosystems, Foster City, CA, USA) was applied to synthesize cDNA from the purified RNA. The miRNA was synthesized using TaqMan miRNA Reverse Transcription kit (Applied Biosystems, Foster City, CA, USA). Moreover, Real Time-Polymerase Chain Reaction was performed by using TaqMan Universal Master Mix II (Applied Biosystems, Foster City, CA, USA) reagent kit and ABI 7500 Fast Real-Time (Applied Biosystems, Foster City, CA, USA). Then, GAPDH (for mRNA) and U6 (for miRNA) were served as the internal references, and the levels of the genes were calculated *via* 2^{-ΔΔCt} method. The primers were as below: TUG1 (Forward: 5'-CTGAAGAAAGGCAACATC-3'; Reverse: 5'-GTAGGCTACTACAGGATTTG-3'); miR-140-5p (Forward: 5'-TGCGGCAGTGTTTTACCCTATG-3'; Reverse: 5'-CCAGTGCAGGGTCCGAGGT-3'); PFN2 (Forward: 5'-CGGCAGAGCTGGTAGAGTCTT-3'; Reverse: 5'-TAGCAGCTAGAACCCAGAGTC-3'); GAPDH (Forward: 5'-GTCAACGGATTTG-TCTGTATT-3'; Reverse: 5'-AGTCTTCTGG-GTGGCAGTGAT-3'); U6 (Forward: 5'-CTC-

GCTTCGGCAGCACATATACT-3'; Reverse: 5'-CGCTTCACGAATTTGCGTGT-3').

Western Blot

The assay was operated as the previous description²⁴. Briefly, the isolated proteins were transfected onto the polyvinylidene difluoride membranes (PVDF; Millipore, Billerica, MA, USA). Subsequently, the membranes were incubated with diluted primary antibodies, including PFN2 (Abcam, Cambridge, MA, USA; ab191054, 1:500) and GAPDH (Abcam, Cambridge, MA, USA; ab181602, 1:10000), and the corresponding secondary antibody (Abcam, Cambridge, MA, USA) was adopted to combine primary antibody. Lastly, an enhanced chemiluminescence kit (Millipore, Billerica, MA, USA) was applied to appear the special protein.

Cell Proliferation Detection

3-(4,5-dimethylthiazol-2-yl)-2,5-diphenyltetrazoliumbromide (MTT) assay was conducted to identify the capacity of the proliferation after MG63 and U2OS cells treated accordingly. Firstly, OS cells were plated into a 96-well plate. After transfection for 48 h, 0.5 µg/mL MTT (10 µL; Promega, Madison, WI, USA) was added into each well. Next, the cell plate was placed into an incubator for 4 h at 37°C, the medium was abandoned immediately, and dimethylsulfoxide (DMSO; Sangon Biotechnology, Shanghai, China) was administered to dissolve the precipitated formazan. The following agitation for 20 min, the optical density of the cell lysate was detected on a microplate reader (Thermo Fisher Scientific, Waltham, MA, USA) at 490 nm.

Transwell Assay

For cell migration assay, transwell chamber (BD Biosciences, Franklin Lakes, NJ, USA) was used for assessing the migration of MG63 and U2OS cells. Firstly, the transfected cells (~8×10⁴ cells/well) were inoculated into the upper chamber with the serum-free medium, and the lower chamber was added with 200 µL complete medium. After incubation for 4 h, the unmigrated cells were scraped using a cotton swab, and the migratory cells were stained using crystal violet (Sangon Biotechnology, Shanghai, China), and next observed and photographed using a microscope (Olympus, Tokyo, Japan). Besides, MG63 and U2OS cells (1×10⁵ cells) were plated into the upper chamber, which was pre-covered with Matrigel

(BD Biosciences, Franklin Lakes, NJ, USA) for cell invasion assay.

Dual-Luciferase Reporter Assay

Partial wildtype or mutant TUG1 fragment containing the binding sites of miR-140-5p, and the common domain between miR-140-5p and wildtype or mutant PFN2 were amplified and then inserted into the Luciferase reporter vector of psiCHECK-2 (Promega, Madison, WI, USA), forming WT-TUG1, MUT-TUG1, WT-PFN2, and MUT-PFN2 reporters. The above reporters were introduced into MG63 and U2OS cells. In the endpoint, the effect of miR-140-5p mimic on the Luciferase activity of the transfected reporters was evaluated by using a Dual-Luciferase reporter assay kit (Promega) on the base of the manufacturer's manuals.

In Vivo Xenograft Model

BALB/c-nude mice (4-6 weeks, n=5/group) were obtained from Shanghai SLAC Laboratory Animal Co., Ltd (Shanghai, China). Above all, the experimental operations were by the Institutional Animal Care and Use Committee of the Yantaishan Hospital. After mice were randomly divided into two groups (sh-TUG1-mediated mice or sh-NC-mediated mice), the stably transfected U2OS cells were injected into the left flank of mice subcutaneously. In the animal experiments, the data of tumor length and width were recorded every 4 days for 6 times. Mice were sacrificed at 27 days post-injection, and the tumors were taken out and weighed.

Statistical Analysis

The data from the three independent assays were displayed as mean ± standard deviation (mean ± SD). Student's *t*-test (for comparisons between two groups) or One-way analysis of variance with Tukey's post-hoc test (for comparisons among three or more groups) was performed to analyze the difference of the data. *p*-value less than 0.05 showed that the difference was statistically significant.

Results

Levels of TUG1 and PFN2 Were Highly Expressed in OS Tissues and Cell Lines

To identify the expression patterns of TUG and PFN2 in the OS progression, the level of TUG1 was determined via qRT-PCR; the results dis-

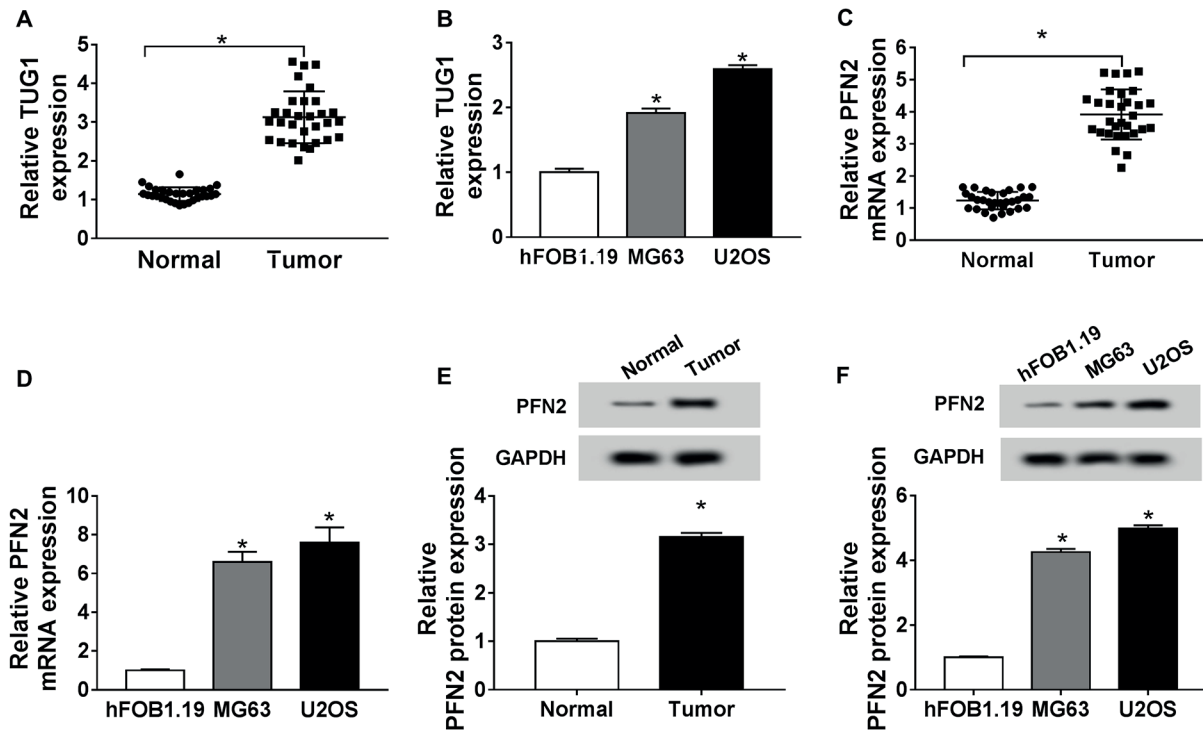


Figure 1. Levels of TUG1 and PFN2 were highly expressed in OS tissues and cell lines. **A-D**, Levels of TUG1 and PFN2 in (**A** and **C**) OS tissues and (**B** and **D**) cell lines were estimated using qRT-PCR. **E** and **F**, The protein expression level of PFN2 was measured by Western blot assay. * $p < 0.05$.

played that TUG1 was highly expressed in OS tissues and cell lines (Figure 1A and 1B). Moreover, the mRNA level of PFN2 was also augmented in OS tumors and cells (Figure 1C and 1D). Simultaneously, we also explored the protein expression of PFN2, and the Western blot analysis discovered that the protein expression of PFN2 was indeed improved in OS tissues and cell lines (Figure 1E and 1F). The data meant that the expression levels of TUG1 and PFN2 were aberrantly intensified in OS tissues and cells.

TUG1 Detection Constrained Proliferation, Migration, and Invasion in MG63 and U2OS Cells

According to the aberrant level of TUG1 in OS, we aimed to explore whether TUG1 participated in the OS development. Firstly, si-TUG1 or si-NC was introduced into MG63 and U2OS cells; the qRT-PCR analysis showed that the transfection of si-TUG1 could clearly hamper TUG1 level *in vitro* (Figure 2A). Subsequently, the effect of TUG1 knockdown on cell proliferation was analyzed using MTT assay; the results suggested

that the proliferation of MG63 and U2OS cells was evidently constrained after transfection with si-TUG1 (Figure 2B and 2C). Meanwhile, TUG1 silencing could especially impede cell migration and invasion in MG63 and U2OS cells (Figure 2D and 2E). The evidence exposed that TUG1 detection could efficiently reduce cell proliferation, migration, and invasion in OS cells.

PFN2 Silencing Curbed Cell Proliferation, Migration, and Invasion In Vitro

Because of the exceptional expression of PFN2 in OS tissues, we guessed that PFN2 acted as a critical role in OS development. To further investigate the role of PFN2 in cell behaviors, the knockdown vector was constructed and introduced into MG63 and U2OS cells, and the mRNA and protein levels of PFN2 were remarkably retarded after transfection with si-PFN2 (Figure 3A and 3B). Subsequently, we explored the impact of PFN2 deficiency on cell proliferation, and MTT analysis exhibited that the ability of cell proliferation was significantly restrained by si-PFN transfection (Figure 3C and 3D). Moreover, the knock-

down of PFN2 markedly blocked the capacity of mobility and invasiveness in MG63 and U2OS cells (Figure 3E and 3F). In brief, the deficiency of PFN2 could notably hinder cell behaviors, including cell proliferation, migration, and invasion in OS cells.

Impact of TUG1 Knockdown on Cell Behaviors was Abolished by Upregulation of PFN2 in OS Cell Lines

Given the repressive role of si-TUG1 and si-PFN2 in OS cell growth, the regulatory mechanism between TUG1 and PFN2 was subsequently investigated. Firstly, the efficiency of pcDNA-PFN2 was verified via qRT-PCR and Western blot assays; the results proved that pcDNA-PFN2 could achieve PFN2 upregulation in the aspects of mRNA and protein (Figure 4A and 4B). Next, si-NC, si-TUG1, si-TUG1+pcDNA-con,

or si-TUG1+pcDNA-PFN2 was transfected into MG63 and U2OS cells, respectively. MTT analysis displayed that the repressive effect of TUG1 detection on cell proliferation was regained via simultaneous transfection with pcDNA-PFN2 *in vitro* (Figure 4C and 4D). Furthermore, the over-expression of PFN2 could rescue the inhibiting role of TUG1 silencing on mobility and invasiveness in OS cells (Figure 4E and 4F). All the data indicated that the effect of TUG1 knockdown on cell behaviors was abrogated by PFN2 upregulation in OS cells.

TUG1 was a Sponge of miR-140-5p to Isolate PFN2

Due to the regulatory mechanism between TUG1 and PFN2 in OS, the specific work pathway of TUG1 was needed to be researched. The prediction of starBase v2 indicated that miR-140-

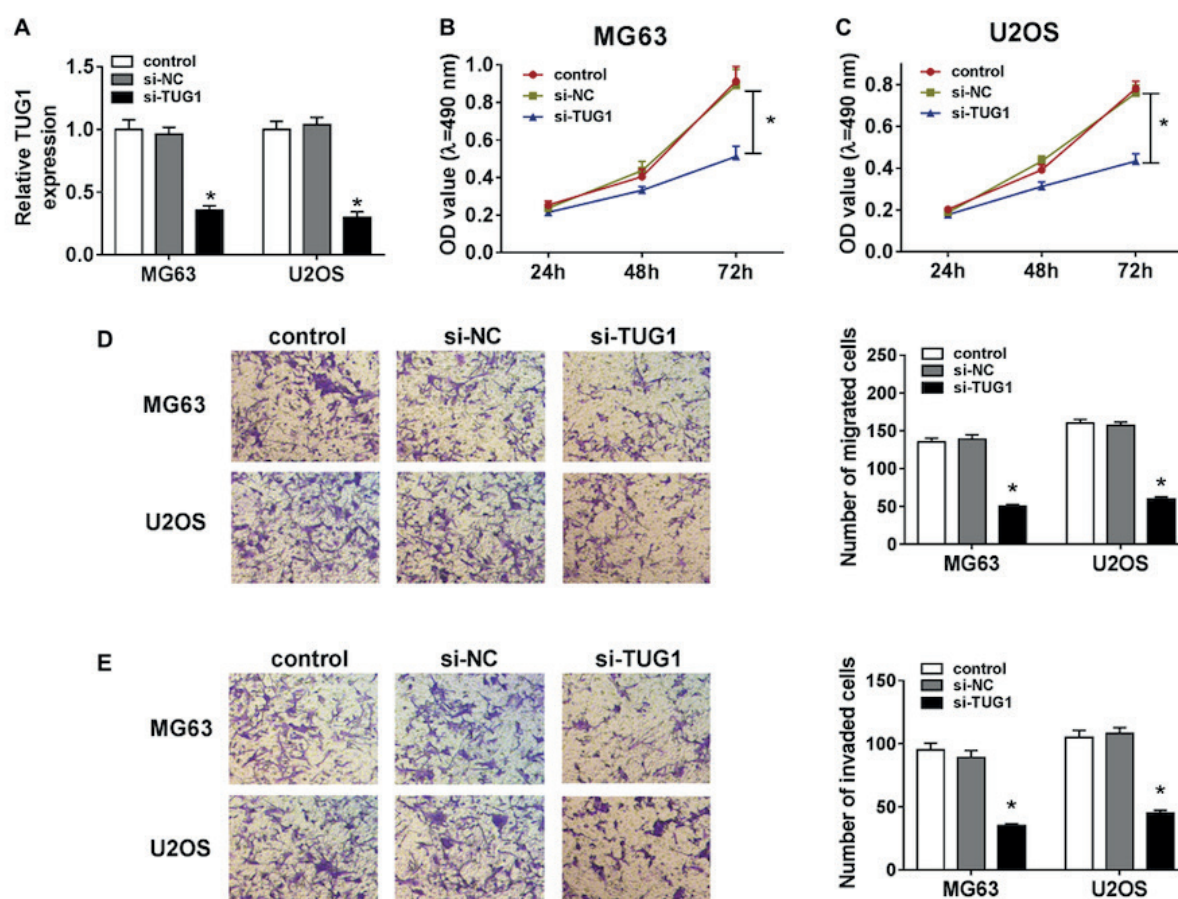


Figure 2. TUG1 detection constrained proliferation, migration, and invasion in MG63 and U2OS cells. MG63 and U2OS cells were transfected with si-TUG1 or si-NC, respectively. **A**, The knockdown efficiency was assessed by qRT-PCR. **B** and **C**, The effect of si-TUG1 on cell proliferation was identified via MTT assay. **D** and **E**, Transwell assay was performed to measure cell migration and invasion in MG63 and U2OS cells (100×). **p*<0.05.

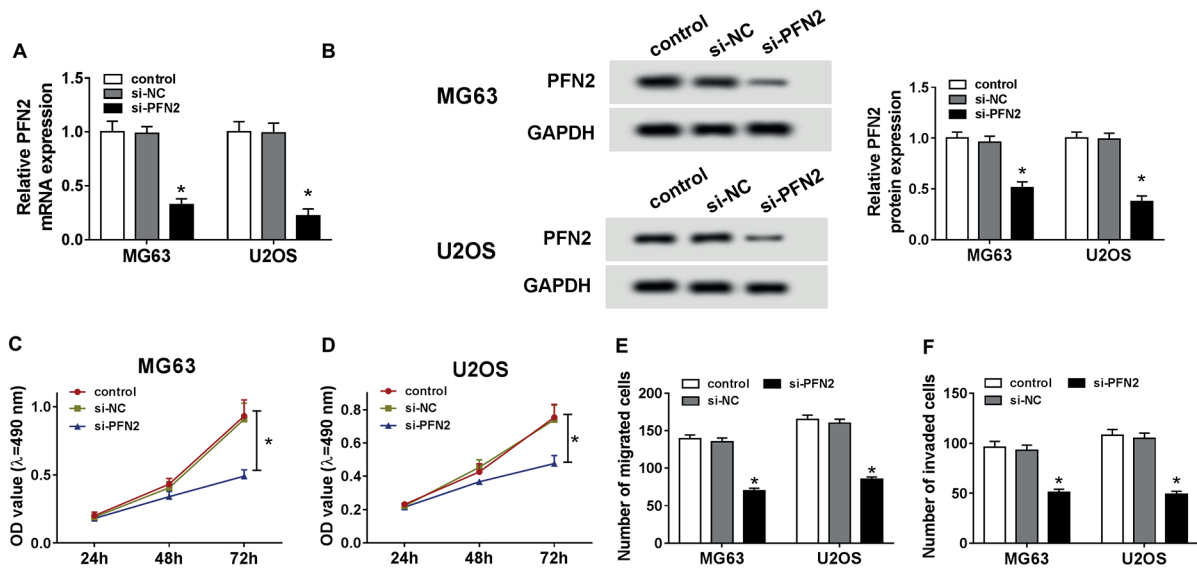


Figure 3. PFN2 silencing curbed cell proliferation, migration, and invasion *in vitro*. Si-PFN2 or si-NC was introduced into MG63 and U2OS cells. **A** and **B**, The mRNA and protein levels of PFN2 were detected utilizing qRT-PCR (**A**) and Western blot assays (**B**), respectively. **C** and **D**, MTT assay was conducted to examine the ability of cell proliferation *in vitro*. **E** and **F**, Cell migration and invasion were measured adopting transwell assay. * $p < 0.05$.

5p was a possible target of TUG1 (Figure 5A). What's more, miR-140-5p mimic could distinctly impede the Luciferase activity of WT-TUG1, but it did not change the luciferase activity of MUT-TUG1 in both MG63 and U2OS cells. The data showed that TUG1 could directly target miR-140-5p (Figure 5B and 5C). After that, qRT-PCR analysis exhibited that the level of TUG1 was opposite with miR-140-5p, showing the acceleratory effect of si-TUG1 and the repressive effect of pcDNA-TUG1 on the level of miR-140-5p in OS cells (Figure 5D). Similarly, we also predicted the interaction between miR-140-5p and PFN2 adopting StarBase v2.0 (Figure 5E). Given the complementary sequences between miR-140-5p and PFN2, WT-PFN2 or MUT-PFN2 was transfected into MG63 and U2OS cells. We found that the inhibitory role of miR-140-5p mimic on the Luciferase activity of WT-PFN2 reporter was rescued after co-transfection with pcDNA-TUG1, while neither miR-140-5p nor pcDNA-TUG1 could significantly change the Luciferase activity in the mutant group (Figure 5F and 5G). Then, qRT-PCR analysis exposed that miR-140-5p mimic drastically retarded the mRNA and protein levels of PFN2, whereas simultaneous introduction of pcDNA-TUG1 could abolish the repressive im-

part of miR-140-5p mimic on PFN2 level (Figure 5H and 5I). In short, TUG1 was a sponge of miR-140-5p to far away PFN2.

Effects of PFN2 Deficiency on Cell Proliferation, Migration, and Invasion were Regained by Either TUG1 Overexpression or miR-140-5p Detection In Vitro

To further explore the role of TUG1, miR-140-5p, and PFN2 in cellular functions of OS, si-NC, si-PFN2, si-PFN2+pcDNA-con, si-PFN2+pcDNA-TUG1, si-PFN2+anti-miR-NC, or si-PFN2+anti-miR-140-5p were introduced into MG63 and U2OS cells, respectively. Firstly, we disclosed that the repressive effect of si-PFN2 on mRNA and the protein levels of PFN2 was overturned *via* synchronously introducing either pcDNA-TUG1 or miR-140-5p inhibitor (Figure 6A-6D). Subsequently, the capacity of cell proliferation was estimated by MTT assay, and the results presented that either TUG1 overexpression or miR-140-5p inhibition could revert the suppressive role of PFN2 detection in the proliferation of MG63 and U2OS cells (Figure 6E and 6F). Similarly, cell migration and invasion, which were markedly curbed by

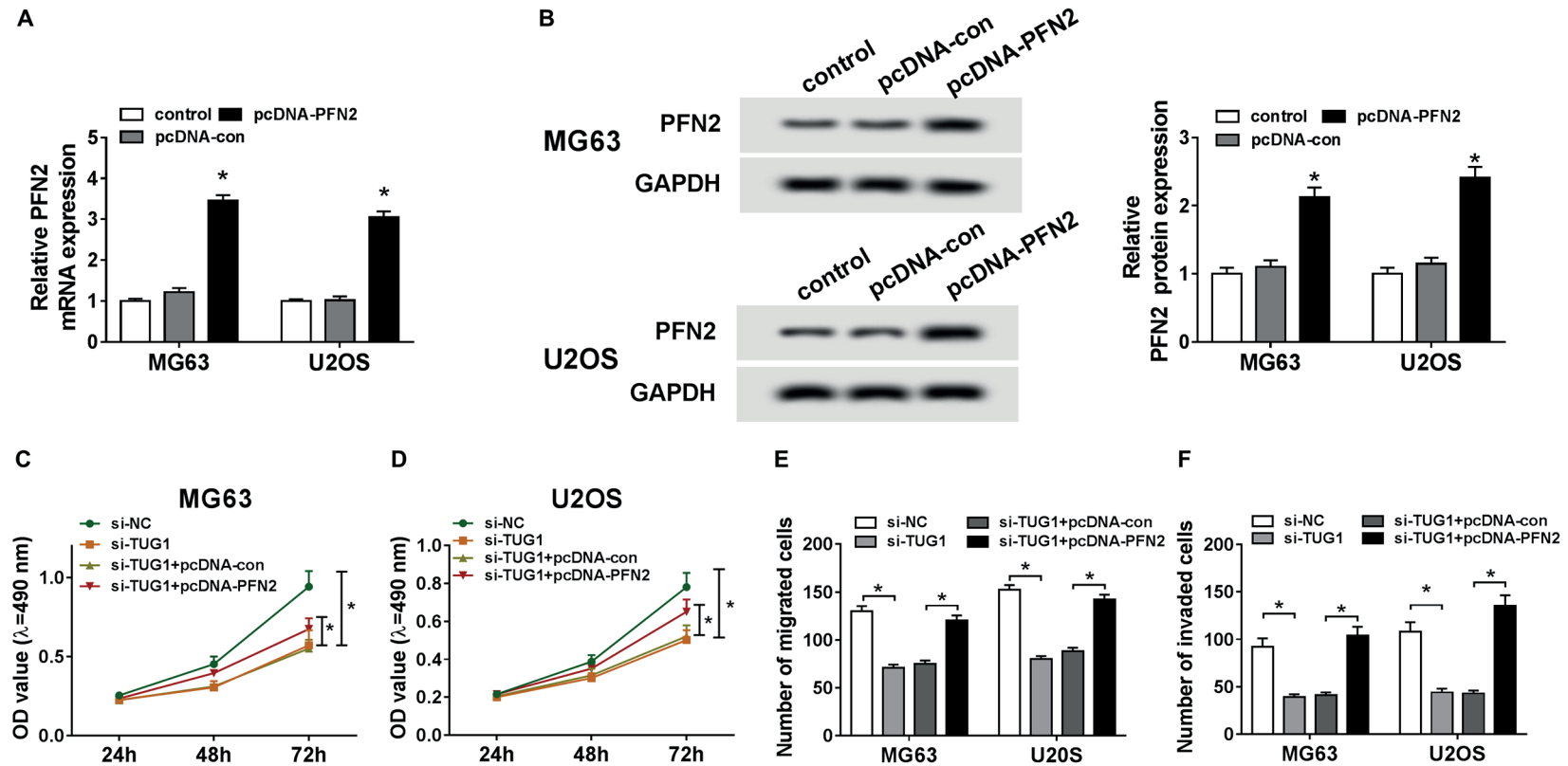


Figure 4. Impact of TUG1 knockdown on cell behaviors was abolished by upregulation of PFN2 in OS cell lines. **A** and **B**, MG63 and U2OS cells were transfected with pcDNA-PFN2 or pcDNA-con, the mRNA and protein levels of PFN2 were determined via qRT-PCR and Western blot assays, severally. **C-F**, Si-NC, si-TUG1, si-TUG1+pcDNA-con, or si-TUG1+pcDNA-PFN2 was introduced into MG63 and U2OS cells. **C** and **D**, The change of cell proliferation was identified utilizing MTT assay. **E** and **F**, Transwell assay was carried out to verify the role of si-TUG1 and pcDNA-PFN2 in cell migration and invasion *in vitro*. * $p < 0.05$.

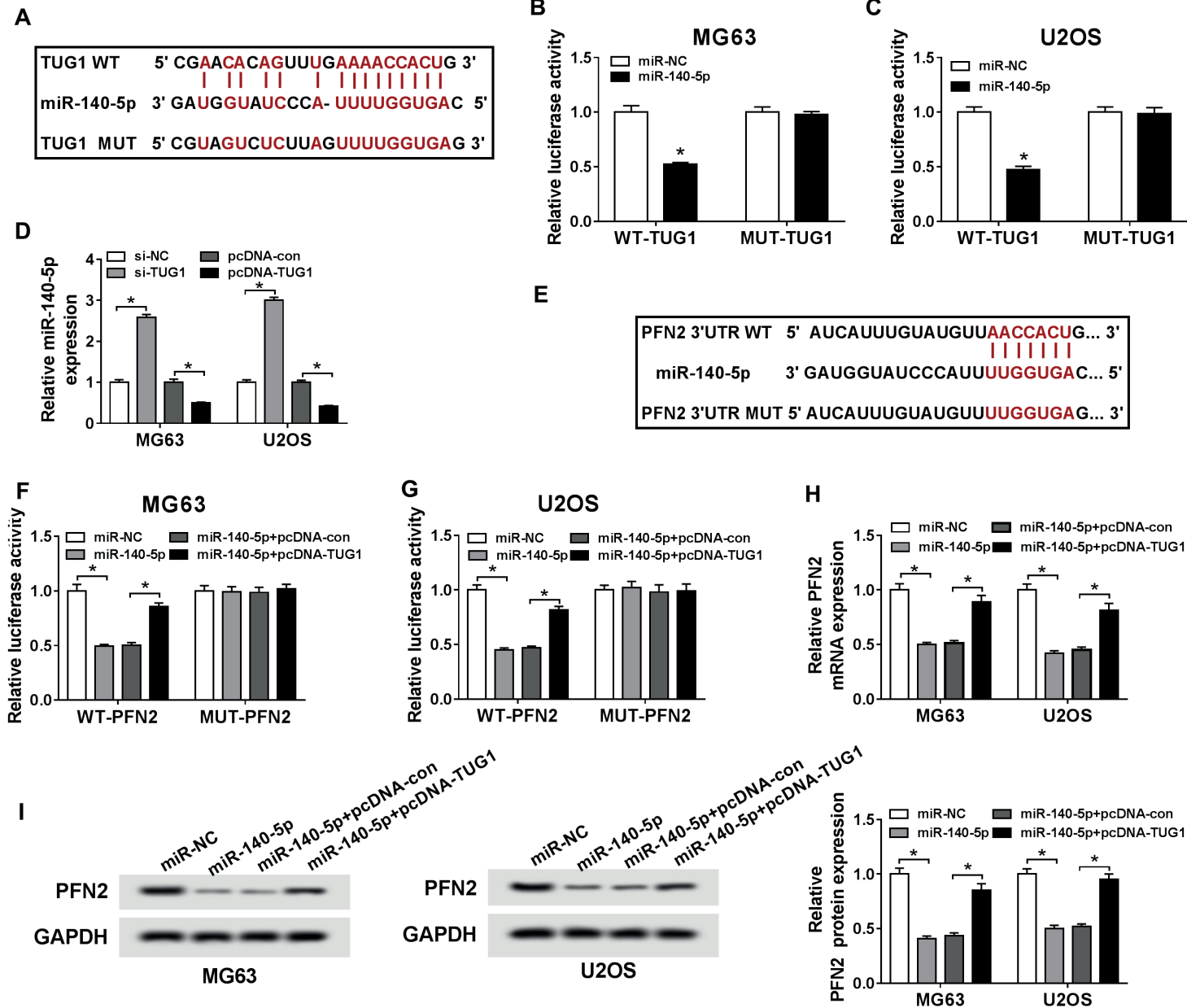


Figure 5. TUG1 was a sponge of miR-140-5p to isolate PFN2. **A**, The complementary sequences between TUG1 and miR-140-5p predicted by starBase v2.0 were shown. **B** and **C**, Luciferase activity of WT-TUG1 or MUT-TUG1 plasmids was determined using dual-luciferase reporter assay. **D**, QRT-PCR was employed to assay the level of miR-140-5p after up-regulation or down-regulation of TUG1 in OS cell lines. **E**, The binding sites between miR-140-5p and PFN2 were predicted using starBase v2.0 software. MiR-NC, miR-140-5p, miR-140-5p+pcDNA-con, or miR-140-5p+pcDNA-TUG1 was introduced into OS cell lines, respectively. **F** and **G**, The Luciferase activities of WT-PFN2 and MUT-PFN2 plasmids were analyzed using dual-luciferase reporter assay. **H** and **I**, QRT-PCR and Western blot assays were used to estimate mRNA and protein levels of PFN2 *in vitro*. * $p < 0.05$.

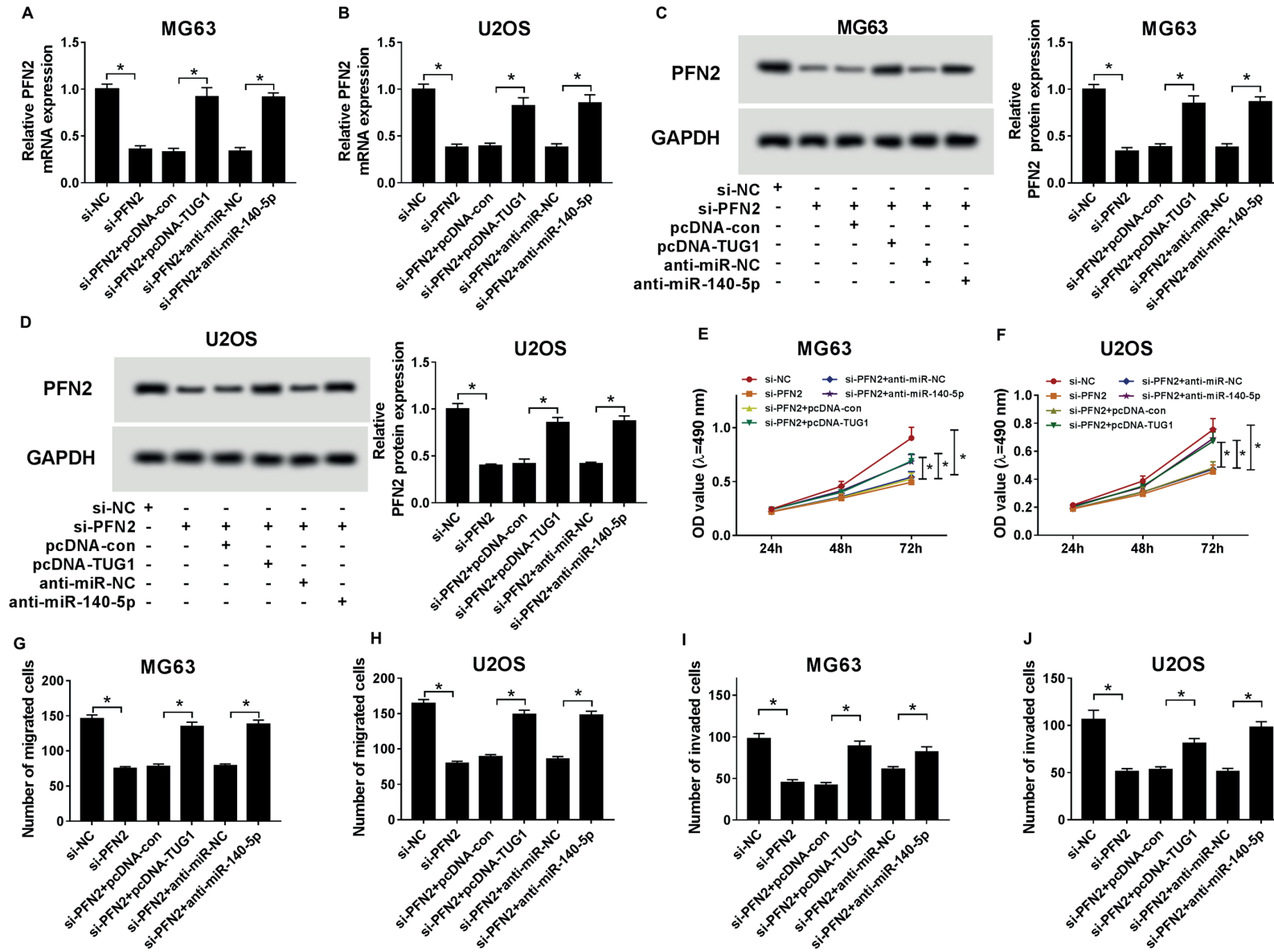


Figure 6. Effects of PFN2 deficiency on cell proliferation, migration, and invasion were regained by either TUG1 overexpression or miR-140-5p detection *in vitro*. MG63 and U2OS cells were transfected with si-NC, si-PFN2, si-PFN2+pcDNA-con, si-PFN2+pcDNA-TUG1, si-PFN2+anti-miR-NC, or si-PFN2+anti-miR-140-5p, (A-D) the mRNA and protein expression levels were analyzed adopting qRT-PCR (A and B) and Western blot assays (C and D), respectively. (E and F) MTT assay was performed to examine cell proliferation in MG63 and U2OS cells. G-J, The capacities of cell migration and invasion were evaluated utilizing transwell assay. **p*<0.05.

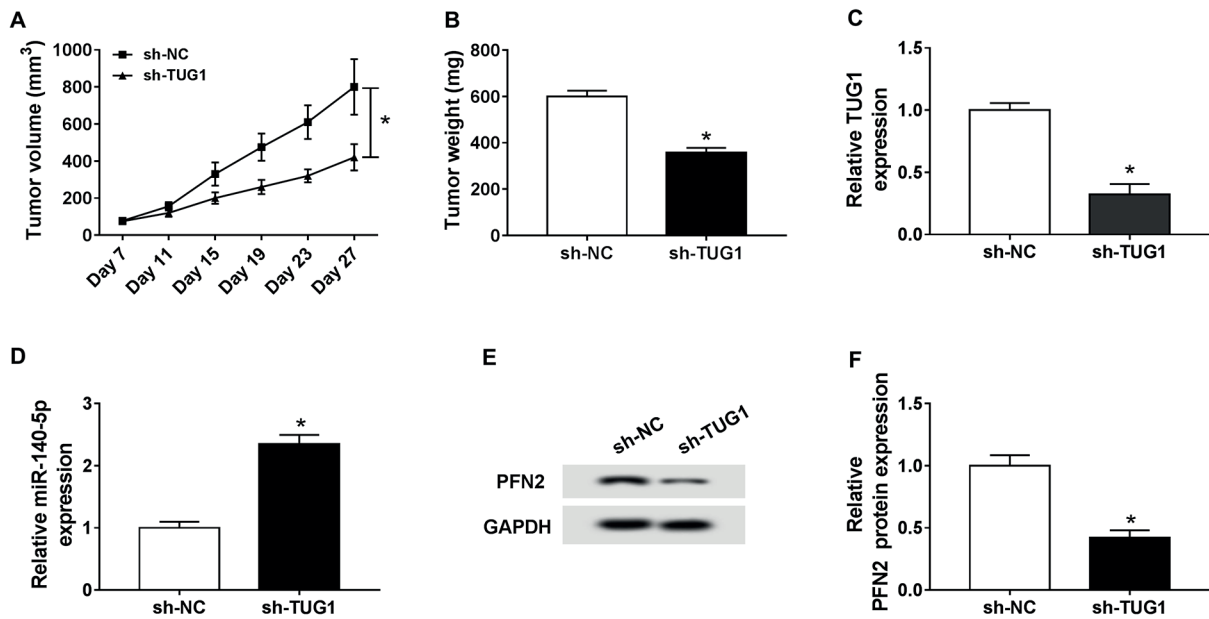


Figure 7. TUG1 detection led to the decrease of OS tumor growth *in vivo*. **A**, Effect of TUG1 silencing on subcutaneous tumor volume was measured. **B**, Tumor weight was measured after mice were sacrificed at 27 days post-injection. **C** and **D**, QRT-PCR was employed to detect the levels of TUG1 and miR-140-5p in xenograft tumor tissues. **E**, and **F**, The protein expression level of PFN2 was analyzed using Western blot. * $p < 0.05$.

PFN2 silencing, were ameliorated by either TUG1 overexpression or miR-140-5p inhibitor *in vitro* (Figure 6G-6J). All the evidence implied that both TUG1 upregulation and miR-140-5p repression could recover the inhibiting effect of PFN2 deficiency on cellular behaviors in MG63 and U2OS cells.

TUG1 Detection Led to the Decrease of OS Tumor Growth In Vivo

To gain insights into the biological role of TUG1 in OS progression, the lentivirus-mediated sh-TUG1 was introduced into U2OS cells to establish stably transfected OS cells. Then, we confirmed that the knockdown of TUG1 could hinder tumor growth, showing as the decrease of tumor volume and weight in the TUG1 deficiency group (Figure 7A and 7B). In addition, the qRT-PCR analysis demonstrated that the level of TUG1 was prominently reduced, while the miR-140-5p level was especially reinforced in the treatment group (Figure 7C and 7D). Finally, the protein expression of mature PFN2 was also identified *via* Western blot assay, and the results expounded that PFN2 protein expression was conspicuously hampered in the sh-TUG1-mediated xenograft tumor tissues

(Figure 7E and 7F). The evidence manifested that TUG1 detection could suppress the tumor growth of OS *in vivo*.

Discussion

OS is a frequent bone tumor with malignancy, seriously affecting the health of human²⁵. lncRNAs, which have been deemed to have no translated proteins sequences, work as the general mediators (suppression or facilitation) in the prognosis and development of human OS²⁶. For example, HNF1A-antisense 1 triggered the growth and invasiveness of OS cells by improving the activation of Wnt/ β -catenin pathway²⁷. Herein, the pathological functions and biological roles of TUG1 in the process and initiation of OS were investigated. Firstly, the qRT-PCR analysis indicated that the TUG1 level was clearly augmented in the OS tissues. In addition, we also exposed that TUG1 deficiency hampered cell proliferation and metastasis in the OS cells, which agreed with earlier evidence²⁸.

Although lncRNAs have been disclosed to be involved in several pathologies, the understand-

ing of their roles remains limited. We firstly implied that TUG1 knockdown indeed constrained cell proliferation, migration, and invasion in MG63 and U2OS cells, whereas the precise regulatory mechanism of TUG1 was needed to be highlighted. Inspired by the ‘competing endogenous RNA (ceRNA)’ regulatory network, we speculate that TUG1 might serve as a ceRNA²⁹. To verify this hypothesis, the bioinformatics analysis showed that miR-140-5p was a probable target gene of TUG1. Subsequent Dual-Luciferase reporter analysis clarified that TUG1 could directly target miR-140-5p in MG63 and U2OS cells. Additionally, earlier records revealed that miR-140-5p curbed metastasis of gastric cancer by targeting YES Proto-Oncogene 1 (YES1)³⁰. Other reports³¹ suggested that miR-140-5p was a target gene of Unigene56159, and its mimic could suppress epithelial-mesenchymal transition in hepatocellular carcinoma cells by acting as ceRNA. With regard to miR-140-5p, it has been broadly emerged to be a vital modulator in diverse malignant tumors. Then, the correlation between miR-140-5p and TUG1 was evaluated *via* qRT-PCR analysis, and the results showed that miR-140-5p level was passively associated with the TUG1 level. Upregulation of TUG1 could decrease miR-140-5p level, whereas the role of si-TUG1 was opposite with pcDNA-TUG1 in regulating miR-140-5p level. Collectively, TUG1 served as a ceRNA of miR-140-5p to modulate the phenotypes of OS cells. Subsequently, we aimed to expose the specific molecular mechanism of miR-140-5p in the process and pathogenesis of OS.

From the above descriptions, we manifested that TUG1 was an oncogenic gene, whereas miR-140-5p acted as a repressive factor in OS development. Then, StarBase V2.0 was employed to search for the potential targets of miR-140-5p, and we uncovered that PFN2 had complementary sequences with miR-140-5p. PFN2, belonging to the PFN family, was present in the brain to regulate neurogenesis and synapse formation *via* interacting with multiple proteins³². In addition, PFN2 could regulate the progression of axonal Charcot-Marie-Tooth disease³³. Despite this, PFN2 was also associated with human cancers and might work as a valuable predictor for the prognosis of head and neck squamous carcinoma³⁴. Of note, the level of PFN2 was co-regulated by TUG1 and miR-140-5p in OS cell lines. Further, the roles of PFN1 silencing in cell behaviors were abrogated by either miR-140-5p

inhibition or TUG1 overexpression. All the data displayed that TUG1 was a sponge of miR-140-5p to isolate PFN2 in OS progression.

Conclusions

Taken together, the knockdown of TUG1 or PFN2 could significantly reduce cell proliferation, migration, and invasion *in vitro*. The effect of TUG1 detection on cell behaviors of OS cells was rescued by either miR-140-5p inhibitor or PFN2 overexpression. Moreover, TUG1 modified the tumor growth *via* miR-140-5p/PFN2 axis in a xenograft tumor model. However, the working pathway of TUG1 in human diseases still needs further researches.

Conflict of Interests

The Authors declare that they have no conflict of interests.

Acknowledgements

This study was supported by the fund of “Health Technology Development Program in Shandong Province (No 2016WS0012)”.

References

- 1) BOTTER SM, NERI D, FUCHS B. Recent advances in osteosarcoma. *Curr Opin Pharmacol* 2014; 16: 15-23.
- 2) CHEN W, ZHENG R, BAADE PD, ZHANG S, ZENG H, BRAY F, JEMAL A, YU XO, HE J. Cancer statistics in China, 2015. *CA Cancer J Clin* 2016; 66: 115-132.
- 3) WU PK, CHEN WM, CHEN CF, LEE OK, HAUNG CK, CHEN TH. Primary osteogenic sarcoma with pulmonary metastasis: clinical results and prognostic factors in 91 patients. *Jpn J Clin Oncol* 2009; 39: 514-522.
- 4) ADAMOPOULOS C, GARGALIONIS AN, PIPERI C, PAPAVASSILIOU AG. Recent advances in mechanobiology of osteosarcoma. *J Cell Biochem* 2017; 118: 232-236.
- 5) SERRA M, HATTINGER CM. The pharmacogenomics of osteosarcoma. *Pharmacogenomics J* 2017; 17: 11-20.
- 6) MA Z, HUANG H, XU Y, HE X, WANG J, HUI B, JI H, ZHOU J, WANG K. Current advances of long non-coding RNA highly upregulated in liver cancer in human tumors. *Onco Targets Ther* 2017; 10: 4711-4717.
- 7) GAO P, WEI GH. Genomic Insight into the role of lncRNA in cancer susceptibility. *Int J Mol Sci* 2017; 18. pii: E1239.
- 8) ADAMS BD, PARSONS C, WALKER L, ZHANG WC, SLACK FJ. Targeting noncoding RNAs in disease. *J Clin Invest* 2017; 127: 761-771.

- 9) YANG G, LU X, YUAN L. LncRNA: a link between RNA and cancer. *Biochim Biophys Acta* 2014; 1839: 1097-1109.
- 10) HU Y, YANG Q, WANG L, WANG S, SUN F, XU D, JIANG J. Knockdown of the oncogene lncRNA NEAT1 restores the availability of miR-34c and improves the sensitivity to cisplatin in osteosarcoma. *Biosci Rep* 2018; 38. pii: BSR20180375.
- 11) YE K, WANG S, ZHANG H, HAN H, MA B, NAN W. Long noncoding RNA GAS5 suppresses cell growth and epithelial-mesenchymal transition in osteosarcoma by regulating the miR-221/ARHI pathway. *J Cell Biochem* 2017; 118: 4772-4781.
- 12) YOUNG TL, MATSUDA T, CEPKO CL. The noncoding RNA taurine upregulated gene 1 is required for differentiation of the murine retina. *Curr Biol* 2005; 15: 501-512.
- 13) ZHANG E, HE X, YIN D, HAN L, QIU M, XU T, XIA R, XU L, YIN R, DE W. Increased expression of long noncoding RNA TUG1 predicts a poor prognosis of gastric cancer and regulates cell proliferation by epigenetically silencing of p57. *Cell Death Dis* 2016; 7: e2109.
- 14) HUANG MD, CHEN WM, QI FZ, SUN M, XU TP, MA P, SHU YQ. Long non-coding RNA TUG1 is up-regulated in hepatocellular carcinoma and promotes cell growth and apoptosis by epigenetically silencing of KLF2. *Mol Cancer* 2015; 14: 165.
- 15) CAO J, HAN X, QI X, JIN X, LI X. TUG1 promotes osteosarcoma tumorigenesis by upregulating EZH2 expression via miR-144-3p. *Int J Oncol* 2017; 51: 1115-1123.
- 16) JIANG L, WANG W, LI G, SUN C, REN Z, SHENG H, GAO H, WANG C, YU H. High TUG1 expression is associated with chemotherapy resistance and poor prognosis in esophageal squamous cell carcinoma. *Cancer Chemother Pharmacol* 2016; 78: 333-339.
- 17) WANG H, YU Y, FAN S, LUO L. Knockdown of long noncoding RNA TUG1 inhibits the proliferation and cellular invasion of osteosarcoma cells by sponging miR-153. *Oncol Res* 2018; 26: 665-673.
- 18) PEREIRA DM, RODRIGUES PM, BORRALHO PM, RODRIGUES CM. Delivering the promise of miRNA cancer therapeutics. *Drug Discov Today* 2013; 18: 282-289.
- 19) JAFRI MA, AL-QAHTANI MH, SHAY JW. Role of miRNAs in human cancer metastasis: Implications for therapeutic intervention. *Semin Cancer Biol* 2017; 44: 117-131.
- 20) JONES KB, SALAH Z, DEL MARE S, GALASSO M, GAUDIO E, NUOVO GJ, LOVAT F, LEBLANC K, PALATINI J, RANDALL RL, VOLINIA S, STEIN GS, CROCE CM, LIAN JB, AQEILAN RI. MiRNA signatures associate with pathogenesis and progression of osteosarcoma. *Cancer Res* 2012; 72: 1865-1877.
- 21) LAN H, CHEN W, HE G, YANG S. MiR-140-5p inhibits ovarian cancer growth partially by repression of PDGFRA. *Biomed Pharmacother* 2015; 75: 117-122.
- 22) WITKE W. The role of profilin complexes in cell motility and other cellular processes. *Trends Cell Biol* 2004; 14: 461-469.
- 23) KIM MJ, LEE YS, HAN GY, LEE HN, AHN C, KIM CW. Profilin 2 promotes migration, invasion, and stemness of HT29 human colorectal cancer stem cells. *Biosci Biotechnol Biochem* 2015; 79: 1438-1446.
- 24) ZHENG J, LIU X, WANG P, XUE Y, MA J, QU C, LIU Y. CRNDE promotes malignant progression of glioma by attenuating miR-384/PIWIL4/STAT3 axis. *Mol Ther* 2016; 24: 1199-1215.
- 25) RITTER J, BIELACK SS. Osteosarcoma. *Ann Oncol* 2010; 21 Suppl 7: vii320-325.
- 26) YANG Z, LI X, YANG Y, HE Z, QU X, ZHANG Y. Long noncoding RNAs in the progression, metastasis, and prognosis of osteosarcoma. *Cell Death Dis* 2016; 7: e2389.
- 27) ZHAO H, HOU W, TAO J, ZHAO Y, WAN G, MA C, XU H. Upregulation of lncRNA HNF1A-AS1 promotes cell proliferation and metastasis in osteosarcoma through activation of the Wnt/beta-catenin signaling pathway. *Am J Transl Res* 2016; 8: 3503-3512.
- 28) YUN-BO F, XIAO-PO L, XIAO-LI L, GUO-LONG C, PEI Z, FA-MING T. LncRNA TUG1 is upregulated and promotes cell proliferation in osteosarcoma. *Open Med (Wars)* 2016; 11: 163-167.
- 29) FANG Z, YIN S, SUN R, ZHANG S, FU M, WU Y, ZHANG T, KHALIQ J, LI Y. miR-140-5p suppresses the proliferation, migration and invasion of gastric cancer by regulating YES1. *Mol Cancer* 2017; 16: 139.
- 30) LV J, FAN HX, ZHAO XP, LV P, FAN JY, ZHANG Y, LIU M, TANG H. Long non-coding RNA Unigene56159 promotes epithelial-mesenchymal transition by acting as a ceRNA of miR-140-5p in hepatocellular carcinoma cells. *Cancer Lett* 2016; 382: 166-175.
- 31) MURK K, WITTENMAYER N, MICHAELSEN-PREUSSE K, DRESBACH T, SCHOENENBERGER CA, KORTE M, JOCKUSCH BM, ROTHKEGEL M. Neuronal profilin isoforms are addressed by different signalling pathways. *PLoS One* 2012; 7: e34167.
- 32) JUNEJA M, AZMI A, BAETS J, ROOS A, JENNINGS MJ, SAVERI P, PISCIOTTA C, BERNARD-MARISSAL N, SCHNEIDER BL, VERFAILLIE C, CHRAST R, SEEMAN P, HAHN AF, DE JONGHE P, MAUDSLEY S, HORVATH R, PAREYSON D, TIMMERMAN V. PFN2 and GAMT as common molecular determinants of axonal Charcot-Marie-Tooth disease. *J Neurol Neurosurg Psychiatry* 2018; 89: 870-878.
- 33) LIU J, WU Y, WANG Q, LIU X, LIAO X, PAN J. Bioinformatic analysis of PFN2 dysregulation and its prognostic value in head and neck squamous carcinoma. *Future Oncol* 2018; 14: 449-459.